Electron Spin Resonance of Free Radicals and Radical Pairs in Irradiated Single Crystal of 1-Methyluracil

Wolfgang Flossmann, Jürgen Hüttermann, Adolf Müller, and Eric Westhof

Lehrstuhl für Physik, Fachbereich Biologie, Universität Regensburg

(Z. Naturforsch. **28 c**, 523–532 [1973]; received April 4, 1973)

Free radicals, radical pairs, 1-methyluracil, monocrystal, ESR-spectra

Radical formation by irradiation with X-rays in single crystals of 1-methyluracil has been measured using ESR-spectroscopy at 9.5 GHz and 35 GHz. When irradiating and measuring at 77 °K radicals characterized by hydrogen abstraction from the methyl group were found to be predominating. For the hyperfine splittings principal values of 8.5 G, 18.2 G, 30.5 G were found for both α-protons and 3.3 G, 2.4 G, 1.7 G for the N(1)-splitting. Pairs of abstraction radicals were also found under these conditions showing quintet splittings of about 10 G and anisotropic dipolar coupling. Average distances parallel to *c* of 6.3 Å and 6.5 Å were found for two types of pairs while those perpendicular to *c* were not analyzed in detail. Irradiating and measuring at room temperature an additional sextet pattern was found in the spectrum and attributed to a radical formed by addition of hydrogen at C(5). For the hyperfine splittings principal values of 8.1 G, 17.5 G, 30.0 G were found for the α-proton and 31.2 G, 34.4 G, 34.1 G for the two equivalent β-protons. Radical concentrations were determined at 77 °K yielding about 90% abstraction radical, 15% of these in pairs and 10% of addition radical. About half of the abstraction radicals are converted to addition radicals between 200 °K and 280 °K. The latter disappear at about 460 °K leaving a fraction of abstraction radicals which is annealed at even higher temperatures.

Radical formation in single crystals of nucleic acid derivatives has been studied with a considerable number of compounds. This work has recently been summarized including some results on 1-methyluracil radicals contained in the present paper [1]. Monoradicals observed in 1-methyluracil after X-irradiation at temperatures between 77 °K and 460 °K have been classified as two different species, types **1** and **2**, characterized by abstraction or addition of atomic hydrogen.

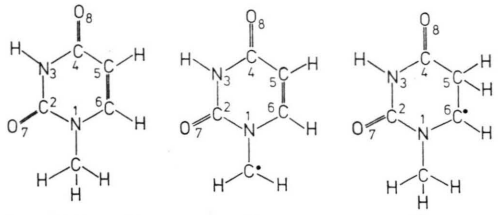

1-methyluracil **1** **2**

These assignments are based on the analysis of splittings, intensities and orientation dependence of hyperfine lines. Under optimal conditions line widths of 1.2 G have been measured, a resolution that has not been achieved with nucleic acid constituents hitherto. Due to the small widths of individual hyperfine lines the anisotropy of splittings could be measured with relatively high accuracy and compared to theory.

At temperatures between 77 °K and 280 °K weak ESR absorption is seen outside the usual range of magnetic field strengths. On account of the observed hyperfine structure the absorption is attributed to interacting pairs of abstraction radicals. This conclusion has been confirmed by the hyperfine structure of the "forbidden" $\Delta m = 2$ transitions observed at half the resonant field strength.

Experimental

1-Methyluracil was purchased from Cyclo Chemical Company and was used without further purification. Colourless, transparent single crystals with well developed faces were grown from saturated aqueous solution by slow evaporation at room temperature.

An analysis of the crystal and the molecular structure has been reported by D. W. Green *et al.* [2]. 1-Methyluracil crystallizes in the orthorhombic system with space group *Ibam* and unit cell dimensions of $a = 13.22$ Å, $b = 13.25$ Å, $c = 6.27$ Å. The crystals resemble needles, elongated along *c*. Although *a* and *b* cannot be distinguished with optical methods because of their small difference in size, they could be assigned to the external configuration using the anisotropy of the splitting constants of the abstrac-

Requests for reprints should be sent to Prof. Dr. A. Müller-Broich, Lehrstuhl für Physik, Fachbereich Biologie, Universität Regensburg, *D-8400 Regensburg 2*, Postfach 397.

tion radical. Four hydrogen bonded pairs of coplanar molecules form a layered structure perpendicular to *c* which contains two magnetically inequivalent molecules giving rise to site splitting in the *ab*-plane (Fig. 1).

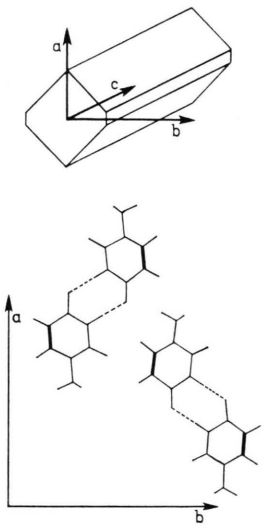

Fig. 1. Crystal structure of 1-methyluracil and relative positions of four molecules in layer parallel to the *ab*-plane constituting one half of an elementary cell.

Single crystals and powder were irradiated with 100 kV X-rays at 77 °K and at room temperature, employing dosages from 150 krad to 80 Mrad. The saturation concentration of the radicals produced at room temperature was of the order of $2 \cdot 10^{17}$ spins per gram using lignite as a reference standard ($3.17 \cdot 10^{17}$ spins per gram).

ESR spectra were registered as first derivatives with a Varian E-9-spectrometer at 9.5 GHz and at 35 GHz. Because of the small line widths of the spectra modulation amplitude and microwave power were carefully reduced until line broadening was completely absent. The crystals were rotated within three mutually perpendicular planes of the *abc*-frame in steps of 6°, using an automatic goniometer described elsewhere [3]. At 77 °K spectra were taken only at 9.5 GHz whereas at room temperature both frequencies were employed.

Annealing experiments in the range of 100 °K – 460 °K were performed with the Varian variable temperature unit. For measurements at 77 °K a liquid nitrogen insert dewar was used. The observed *g*-factors were measured at 35 GHz using DPPH ($g = 2.0036$) as a standard.

Results and Discussion

Abstraction radical **1**

After irradiation of single crystals at room temperature abstraction and addition radicals of types **1** and **2** give rise to a complex composite ESR spectrum. Annealing for about 20 min at 200 °C or storage for about two months at room temperature greatly simplifies the spectral pattern indicating the survival of the abstraction radical only.

The same spectrum is also seen after irradiation at 77 °K. At this temperature additional lines from interaction between pairs of radicals are also present. On warming up, the latter disappear at about 0 °C (280 °K) simultaneously with a large fraction of isolated abstraction radicals. The quantitative results will be discussed below in greater detail.

After irradiation at 77 °K a yellow colouring of the originally transparent crystals was obtained changing into a darker brown at very high doses. The colour disappeared on warming up parallel to the decay of abstraction radicals around 460 °K.

ESR spectra of the abstraction radical measured at 9.5 GHz and at room temperature after annealing at 200 °C are shown in Fig. 2. When the magnetic

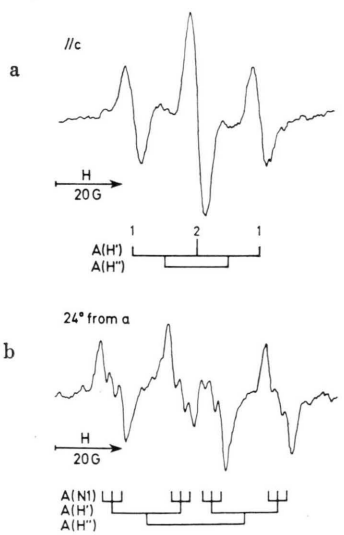

Fig. 2. ESR spectra of X-irradiated single crystal annealed at 200 °C and measured at room temperature using 9.5 GHz, with orientation of magnetic field: a. parallel to axis *c* showing two equivalent H_α-couplings; b. normal to axis *c* showing two different H_α-couplings and one *N*-coupling.

field is parallel to the *c*-axis a wide triplet of intensity ratio 1:2:1 is seen. The individual lines are further split into triplets of equal intensities. A trip-

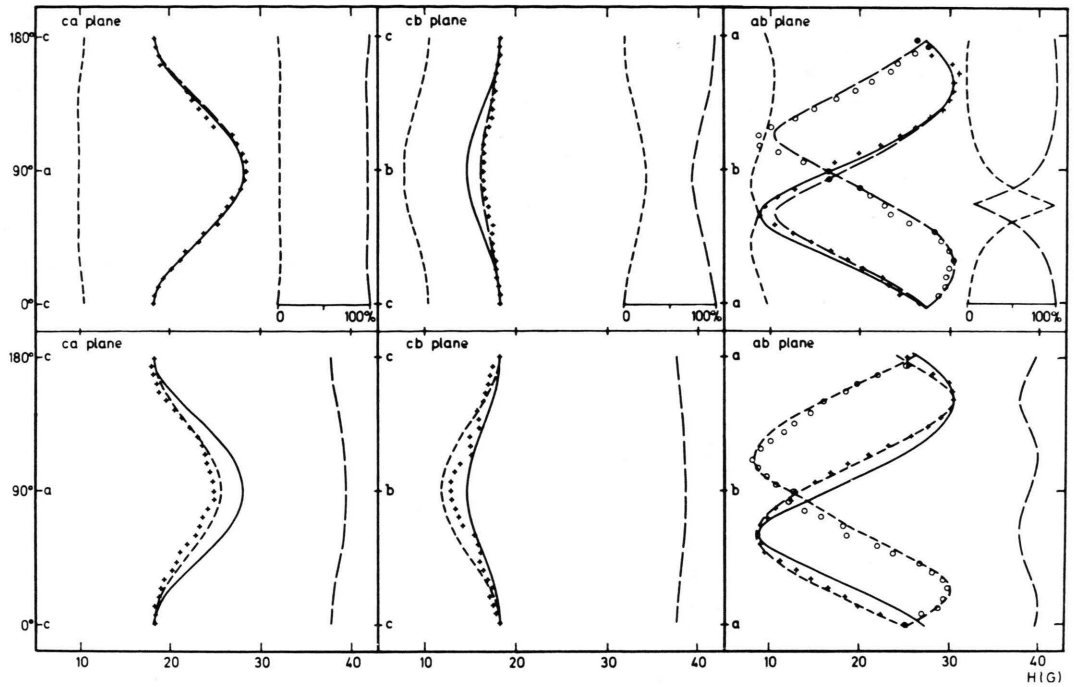

Fig. 3. Angular variation of the two major doublet splittings in ESR spectra of X-irradiated single crystals at room temperature after annealing at 200 °C. Experimental points (crosses) are shown in three orthogonal planes at 9.5 GHz (top) and 35 GHz (bottom) and compared to various theoretical curves: 1. First order approximation neglecting the nuclear Zeeman-term (full lines) and 2. "inner" and "outer" doublets obtained by inclusion of the nuclear Zeeman-interaction in the spin Hamiltonian (broken lines). For each plane at 9.5 GHz (top) theoretical intensities for "inner" and "outer" doublets have been inserted. In the *ab*-plane only the one theoretical curve giving best fit is drawn for the set of experimental points (circles) due to the second proton, while the other two theoretical curves are shown for one proton only.

let of 1:2:1 intensity ratio as along *c* is also seen along the *a*- and *b*-axis but in the latter orientation the additional triplet splitting is better resolved. At intermediate angles double pairs of triplets have been registered (Fig. 2 b).

H_α-splitting

The complete orientational variation of the strongly anisotropic α-proton splittings measured at 9.5 GHz and at 35 GHz is shown in Fig. 3. It may be noted that the experimental points are closely following those theoretical curves that include the nuclear Zeeman-term and represent the splitting of highest theoretical intensity. Very poor fit is obtained between experiment and theory when this factor is neglected. Such behaviour must be expected from our data since the α-coupling is comparable to twice the nuclear Zeeman-energy at most orientations even at 9.5 GHz. The theoretical results yield a splitting of the first order doublet into "inner" and "outer" doublets when the nuclear Zeeman-term is included. At 9.5 GHz the bulk of the total intensity is usually contained in the "outer" doublet (Fig. 3, top), whereas the reverse is true at 35 GHz in all orientations, hence the relative intensities have been omitted in the lower half of Fig. 3. The only irregularity is seen in the *ab*-plane at 9.5 GHz where the relative intensities are crossing near the particular orientation giving minimum splitting. At this angle the expected transition of the experimental points from the "outer" to the "inner" doublet is visible.

In order to obtain the characteristic spectral data shown in Table I a least squares fit was employed in the first order approximation initially. Using the resulting principal values of the coupling tensor and the direction cosines the theoretical curves including the nuclear Zeeman-term were calculated following the concise treatment of Farach and Poole [4] and compared to the experimental points. Finally, the characteristic values were modified until optimal fit in the three orthogonal planes was reached. The angle between the bonds of the two α-protons and the C_α-atom was found to be 126° by this procedure and not 120° as would be expected for pure sp^2

Table I. Principal values and direction cosines of the nuclear coupling constants and the *g*-tensor of the abstraction radical.

	Component	Principal values Experimental	Theoretical	Direction cosines *a*	*b*	*c*	Direction in radical
A(H′)	anisotropic	-11.4 ± 0.5 G	-11.0 G	0.87	+0.50	0.00	⊥ C-H′-bond
		$+10.6 \pm 0.5$ G	$+9.8$ G	−0.50	0.87	0.00	∥ C-H′-bond
		$+0.9 \pm 0.5$ G	$+1.1$ G	0.00	0.00	1.00	∥ p_z-orbital
	isotropic	-19.1 ± 0.5 G					
A(H″)	anisotropic	-11.4 ± 0.5 G	-11.0 G	0.91	+0.41	0.00	⊥ C-H″-bond
		$+10.6 \pm 0.5$ G	$+9.8$ G	−0.41	0.91	0.00	∥ C-H″-bond
		$+0.9 \pm 0.5$ G	$+1.1$ G	0.00	0.00	1.00	∥ p_z-orbital
	isotropic	-19.1 ± 0.5 G					
A(N)	anisotropic	$(-)0.1 \pm 0.5$ G					∥ C-N-bond
		$(+)0.8 \pm 0.5$ G					⊥ C-N-bond
		$(-)0.8 \pm 0.5$ G					∥ p_z-orbital
	isotropic	$(+)2.5 \pm 0.5$ G					
g		2.0031 ± 0.0002					∥ C-N-bond
		2.0028 ± 0.0002					⊥ C-N-bond
		2.0018 ± 0.0002					∥ p_z-orbital

hybridisation. The theoretical principal values indicated in Table I were calculated using the derivation of McConnell and Strathdee [5] and the following values for the characteristic parameters: $Z_{\text{eff}} = 2.9$, $R(\text{C}-\text{H}) = 1.02$ Å, $\varrho(\text{C}) = 0.76$.

Contrary to radical **2** discussed below, "inner" and "outer" lines of radical **1** have never been observed simultaneously in one spectrum. This is partly due to the presence of an additional triplet splitting and partly to the larger widths of individual hyperfine lines of the latter which vary between 1.6 and 2.1 G.

Nitrogen splitting

When the doublet splittings discussed above are taken into account, the 1:1:1 triplet shown in Fig. 2 b is left over. A maximum splitting is found when the magnetic field is parallel to *b* and a minimum parallel to *c*. In the latter case the hyperfine lines are not well resolved but they can be deduced from the resulting line broadening of 4.6 G (Fig. 2 a) when the width of the single lines is assumed to be about 1.6 G, that is, close to the maximum value found in other orientations.

The observed angular dependence of the total nitrogen splitting can be separated into an isotropic part and a smaller anisotropic part and is explained by interaction of the unpaired spin density with the N(1) nucleus. It can be divided into three parts: 1. Unpaired spin density at N(1), 2. dipole-dipole interaction, and 3. spin polarisation. Assuming probable contributions [6, 7], satisfactory agreement between theoretical and experimental data can be achieved. Crossing of nitrogen hyperfine lines due to a change in the sign of the nuclear coupling has been discussed on theoretical grounds [6]. In our case, line crossing should be excluded owing to the fact that the minimum total width seen in any orientation is much larger than that of a single line.

Structure of radical **1**

From the characteristic spectral data compiled in Table I the following radical structure has been deduced. The unpaired electron is mainly localized on a carbon nucleus interacting with two equivalent α-protons and a nitrogen atom in accord with the structure of type **1** radicals.

Further support to this assignment is given by the orientations associated with the principal values of the hyperfine tensors. These are close to those expected from crystallographic data. Hence, it is concluded that radical formation is not accompanied by major molecular rearrangements.

The fact that the α-protons are not equivalent in all orientations shows that the radical group is not rotating freely even at room temperature. A similar conclusion was reached for methylene radical groups in other bases, *i. e.* 9-methyladenine [8], 5-methylcytosine [9], thymine [10] and 6-azathymine [11].

From the equivalence of the two protons when the magnetic field is directed parallel to *c*, it further follows that the two CH bonds are normal to that axis, *i. e.* parallel to the plane of the ring. In contrast to the findings of Schmidt and Snipes [8] the proton

coupling was found to be independent of temperature between 77 °K and 300 °K.

The principal values of the g-tensor given in Table I are those of a typical carbon radical and therefore support the chosen assignment.

Assuming a theoretical splitting of $Q = -25$ G for a proton in α-position relative to a carbon atom carrying 100% spin density in a π-orbital the observed isotropic value of 19.1 G results in a spin density of $\varrho = 0.74$. The remainder of about 30% is distributed over the ring system, predominantly at N(1), C(2) and O(7).

Radical pairs

After irradiation of single crystals with X-rays at 77 °K relatively weak but distinct lines are found far beyond the usual range of ESR absorption of organic radicals (Fig. 4). These patterns are strongly anisotropic as shown in Fig. 5 indicating the presence of radical pairs. If this interpretation is correct, "forbidden" transitions characterized by $\Delta m = 2$ should occur at about half the resonant field strength. Such an absorption was indeed observed with irradiated powder as well as with single crystals (Fig. 6).

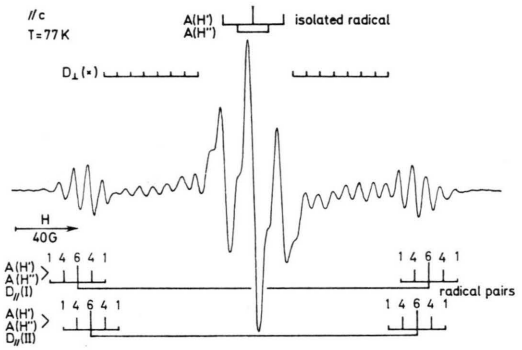

Fig. 4. ESR spectrum of X-irradiated single crystal at 77 °K with magnetic field parallel to the c-axis showing triplet of the abstraction radical and additional anisotropic splittings attributed to pairs of abstraction radicals.

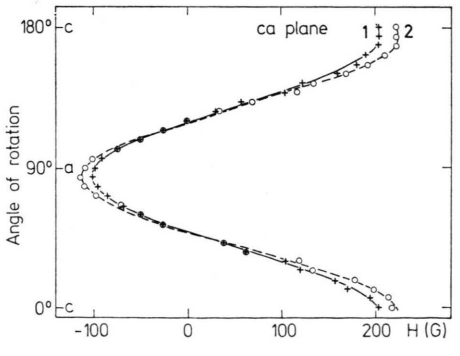

Fig. 5. Angular variation of the dipolar splitting due to radical pairs in the *ca*-plane with magnetic field normal to the *b*-axis. The curves shown have been calculated theoretically with the parameters listed in Table II.

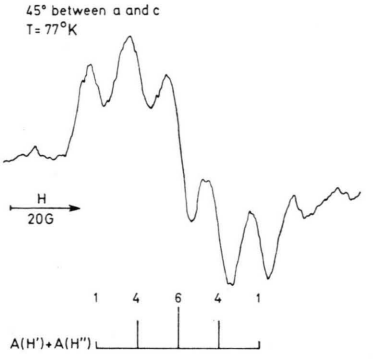

Fig. 6. ESR spectrum of X-irradiated single crystal oriented at an angle of 45° between c and the magnetic field, measured at half the resonant field and 100 °K, showing quintet splitting of $\Delta m = 2$ transitions.

Composition

In the half-field spectrum at $g = 4$ the dipolar coupling is absent. Hence, the hyperfine structure under these conditions is the same as that of a pair of monoradicals with the same orientation relative to the magnetic field but irrespective of their mutual orientation and distance. The spectrum shown in Fig. 6 was obtained with a single crystal oriented at 45° between the magnetic field and the crystal axis c. It is characterized as a quintet of nearly binomial intensity distribution and a splitting of about 12 G. A quintet was also found with a polycrystalline sample. Due to the random orientation of radical pairs the individual lines were broadened in this case.

From the observed spectra at $g = 4$ it is concluded that the radical pairs observed are composed of pairs of abstraction radicals only. As will be shown below, a small fraction of addition radicals (about 10%) is present after irradiation at 77 °K. These have not been found in the hyperfine structure at $g = 4$ and hence cannot contribute significantly to the formation of radical pairs. This result is consistent with the spectra observed at $g = 2$ since all the numerous hyperfine lines which have been resolved under these conditions in addition to those of the monoradicals can be attributed to pairs of abstraction radicals differing in spatial arrangement only. The latter are

characterized in Fig. 4 by the regular spacing of hyperfine lines and their strong orientation dependence. Again, the splitting of about 9 G is the same as half that of the abstraction radical in the same orientation. The latter is indicated at the top of Fig. 4 while all others except the dipolar splittings are due to radical pairs.

Spatial arrangements

Different hyperfine lines attributed to radical pairs can be combined into groups of identical orientational variation. The number of groups and their relative intensities depend on the dose of radiation and can be modified by annealing. Usually, spectra are less complicated at lower doses and higher temperatures but these changes have not been investigated extensively. It has been found, however, that the radical pairs disappear completely parallel to a transformation of abstraction radicals into addition radicals when the temperature is raised to 280 °K. This observation supports the conclusion that the radical pairs observed are composed of abstraction radicals.

The orientation dependence of two groups of hyperfine lines indicated by bars at the bottom of Fig. 4 has been analyzed in detail on account of their favourable intensities in comparison to other groups. The outer quintets are attributed to two types of radical pairs, **1** and **2**, the latter being about 50% more abundant. The variation of these lines in the *ca*-plane is shown in Fig. 5. Experimental points representing the centre of each group have been fitted to the function

$$D = 3\,\beta\, r^{-3}\,(3\cos^2\Theta - 1)$$

yielding the values listed in Table II. It is seen that both the maximum splittings in this plane occur at the same angle close to *c*, the deviation of about 6° being possibly due to misorientation of the crystal.

Table II. Principal values of the dipolar coupling tensor and average unpaired spin separation *r* for the predominating radical pairs in 1-methyluracil.

	Principal values	Unpaired spin separation
pair **1**	$D_{\parallel} = 204 \pm 2$ G $D_{\perp} = -102 \pm 2$ G	6.49 Å
pair **2**	$D_{\parallel} = 224 \pm 2$ G $D_{\perp} = -112 \pm 2$ G	6.27 Å

From the minimum values of the splittings $D_{\perp}$ characteristic distances *r* for the dipolar interaction can be calculated independent of a possible misorientation applying the formula

$$D_{\perp} = -3\,\beta\, r^{-3}.$$

The values obtained are both very close to the length of the crystallographic unit cell of 6.27 Å along *c* as it is shown in Fig. 7. In the assumed configuration the two radicals of a pair are situated in different molecular planes which are separated by an intermediate layer of non-radical molecules perpendicular to *c*. The latter are shifted not only along *c* but also horizontally parallel to *a* and *b*. Prior to radical formation the pyrimidine rings of the parent molecules are coplanar to the molecular layers and thus perpendicular to *c*.

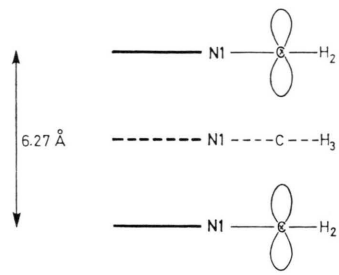

Fig. 7. Spatial arrangement of radical pairs in layers of single crystals. The double distance between neighbouring layers (length of elementary cell) parallel to *c* from crystallographic data is shown on the left. The non-radical molecule (broken lines) is situated intermediate between upper and lower layers but is shifted horizontally along the *a* and *b* axes with respect to neighbouring molecules.

From the observation that mainly the inner quintet attributed to radical pair **2** is found at relatively low radiation doses (about 8 Mrad) it is concluded that the corresponding average distance of 6.5 Å is that adopted by radical pairs in the original crystal order. The small excess above the length of the unit cell of 6.27 Å may be due to a systematic difference between the two or, if real, to a molecular rearrangement on radical formation (note added in proof)*. The outer group is visible only at very high doses (about 80 Mrad) when the crystal lattice has suffered substantial radiation damage. Under these conditions an average distance of 6.3 Å, equal to the length of the unit cell, is obtained. Since the unpaired spins cannot be localized with great precision the absolute values of average distances are subject to corresponding uncertainties. Hence, significance can be attached much less to the absolute values of average distances than to their difference.

In addition to the splittings $D_{\|}$ (**1**) and $D_{\|}$ (**2**) further dipolar splittings of about 9 G can be seen in Fig. 4. These have been designated $D_{\perp}$(*) and are attributed to radical pairs in the *ab*-plane. Due to interference between several different groups with relatively small intensities these have not been analyzed in detail. For the reasons given above they are assumed to be composed of abstraction radicals as well.

Addition radical **2**

The ESR spectrum attributed to a second type of radical, the addition radical **2**, can be annealed by heating to 200 °C but has not been obtained free of the abstraction radical **1**. The former spectra can still be analyzed due to their larger total width. For this purpose optimal conditions were found after irradiation at room temperature. An example taken at 9.5 GHz with the magnetic field parallel to *c* is shown in Fig. 8. At the given orientation a sextet is seen composed of a triplet of doublets which are split still further by minor couplings.

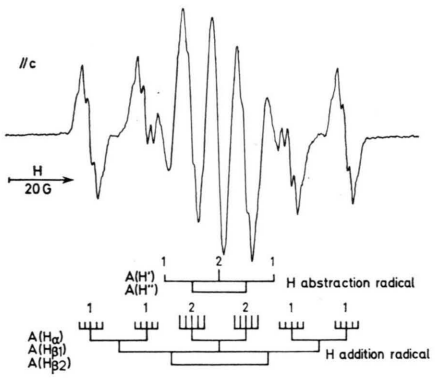

Fig. 8. ESR spectrum of X-irradiated single crystal at room temperature with magnetic field parallel to the *c*-axis showing superposition of triplet (above) and sextet (below) composed of one H_{α}-coupling and two H_{β}-couplings. Additional splittings into quintets is also indicated.

H_{β}-splitting

The basic triplet splitting has a value of about 33 G and is nearly isotropic. Hence, it is attributed to two equivalent β-protons. The widths of individual lines which was found to be as small as 1.2 G in some orientations, permitted to analyze the weak orientation dependence of the β-coupling. Experimental points shown in Fig. 9 have been fitted to the

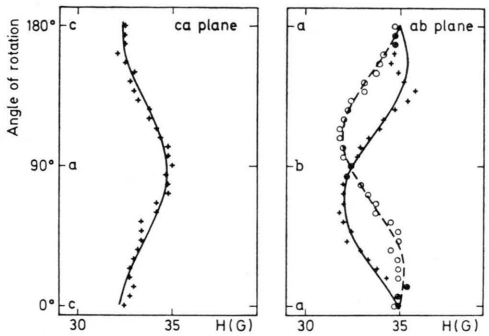

Fig. 9. Anisotropy of the two equivalent β-protons in hydrogen addition radical observed at 9.5 GHz and room temperature.

function

$$A^2(\Theta) = P\cos^2\Theta + Q\sin^2\Theta - 2\,\mathrm{R}\sin\Theta\cos\Theta$$

by the least squares method [4]. The principal values obtained are listed in Table III. The calculation of the anisotropic coupling tensor of the β-protons was executed following the method of Derbyshire [12].

Spin polarization of bonds has been neglected on account of its small contribution of about 3 per

Table III. Principal values and direction cosines of the nuclear coupling constants and the *g*-tensor of the addition radical.

	Component	Principal values Experimental	Theoretical	Direction cosines *a*	*b*	*c*	Direction in radical
$A(H_{\alpha})$	anisotropic	-11.4 ± 0.5 G	-10.5 G	0.81	± 0.59	0.00	$\perp$ C(6)-H-bond
		$+10.5 \pm 0.5$ G	$+9.4$ G	∓ 0.59	0.81	0.00	$\|$ C(6)-H-bond
		$+0.9 \pm 0.5$ G	$+1.0$ G	0.00	0.00	1.00	$\|$ p_z-orbital
	isotropic	-18.6 ± 0.5 G					
$A(H_{\beta})$	anisotropic	$+2.0 \pm 0.5$ G	$+2.3$ G	0.93	± 0.37	0.01	along the bisector of the H′-C(5)-H″-angle
		-1.2 ± 0.5 G	-1.2 G	∓ 0.37	0.91	± 0.14	$\perp$ both directions
		-0.9 ± 0.5 G	-1.0 G	0.04	∓ 0.14	0.99	$\|$ p_z-orbital
	isotropic	$+33.2 \pm 0.5$ G					
g		2.0030 ± 0.0004		Cylindrically symmetric			$\|$ molecular plane
		2.0020 ± 0.0004					$\perp$ molecular plane

cent [13]. The following parameters were used in the calculations:

$$Z_{\text{eff}} = 2.9,\ R(\text{C}-\text{C}) = 1.47\ \text{Å},\ R(\text{C}-\text{H}) = 1.09\ \text{Å},$$
$$\varrho(\text{C}_\alpha) = 0.7\,.$$

For the β-carbon atom an sp^3-conformation was assumed.

Doublet splitting

The additional doublet splitting found in the spectrum is strongly anisotropic and is complicated by site splitting and second order lines both predominating in the *ab*-plane. The experimental values for the splitting in the three orthogonal planes at 9.5 GHz and at 35 GHz are shown in Fig. 10 in comparison to theoretical curves. As has been found with the abstraction radical the fit of experimental points to theoretical curves is improved significantly when the nuclear Zeeman-term is included. In some orientations nearly parallel to *a* or *b*, both the "outer" and "inner" splittings can be found in the same spectrum.

Relative intensities for the spectra taken at 9.5 GHz have been inserted in the upper half of Fig. 10. As has been demonstrated above for the abstraction radical at 9.5 GHz the higher intensity is correlated to the "outer" doublet with the exception of a limited region in the *ab*-plane where this relation is reversed. At 35 GHz the "inner" doublet is more intense in any orientation. Hence, the corresponding curves have been omitted.

The theoretical values used to calculate the curves are shown in Table III together with the theoretical principal values for H_α and H_β. The procedure of McConnell and Strathdee [5] was used as for the abstraction radical with the same parameters except a slightly reduced spin density of $\varrho = 0.73$ at C(6).

In the *ab*-plane, site splitting is observed in agreement with crystallographic data (Fig. 1). For simplification only one set of theoretical curves was drawn for the two types of magnetically inequivalent molecules.

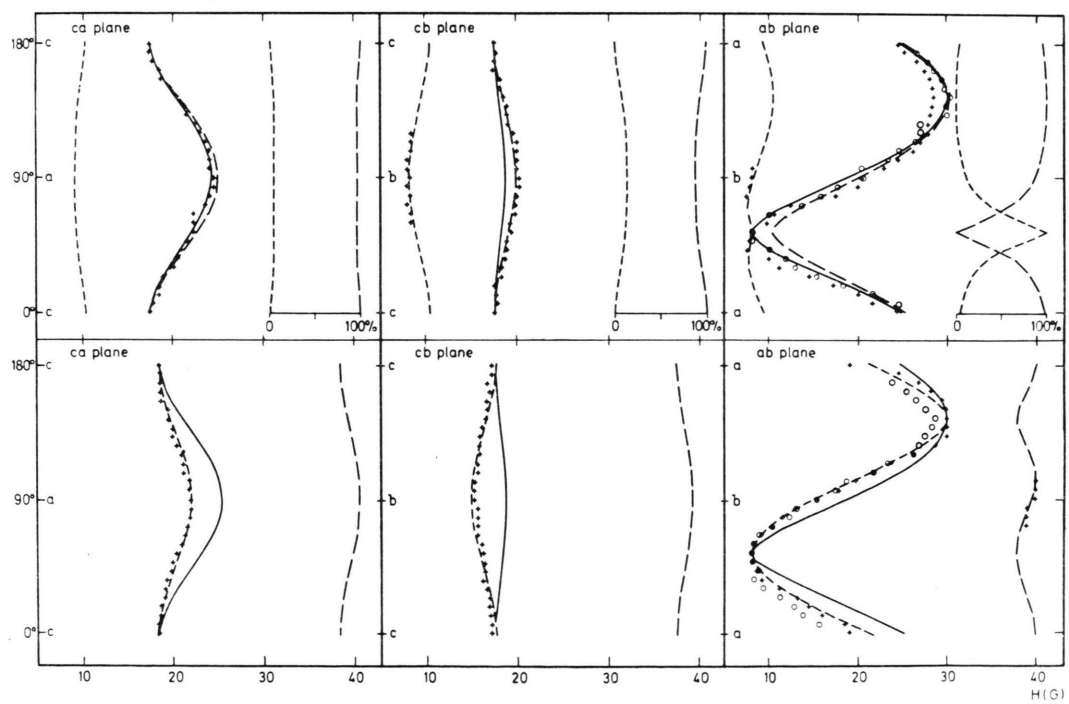

Fig. 10. Angular variation of the anisotropic doublet splitting contained in the sextet spectrum at room temperature in three orthogonal planes at 9.5 GHz (top) and 35 GHz (bottom) showing experimental points and various theoretical curves: **1.** Neglecting the nuclear Zeeman-term (full lines) and 2. "inner" and "outer" doublets obtained by inclusion of nuclear Zeeman-interaction in the spin Hamiltonian (broken lines). For each plane at 9.5 GHz (top) theoretical intensities for "inner" and "outer" doublets have been inserted. In the *ab*-plnae the two sets of experimental points represented by crosses and circles are due to site splitting.

Minor splittings

Parallel to the *b*-axis a 1:1:1 triplet of about 2.5 G splitting can be identified at 9.5 GHz and 35 GHz which is attributed to nitrogen interaction. At other orientations superposition of further splittings results in up to six lines which show a complicated pattern of orientation dependence. An example is given by the quintet indicated in Fig. 8 where second order lines are absent. The pattern found is attributed to the combined interactions of N(1) and the γ-protons of the methyl group. A comparison of spectra taken at 9.5 GHz and at 35 GHz shows that second order effects are also present at orientations other than *c*. At a reduced temperature (77 °K) distinct variations of spectral structures occured resulting in reduced resolution in case of the quintet of Fig. 8. These observations suggest that free rotation of the methyl group is slowed down. It has not been possible, however, to separate the methyl splitting from that of the N(1) atom and a detailed analysis of these splittings has not been accomplished.

Structure of radical **2**

The characteristic spectral data are listed in Table III. The existence of two equivalent β-protons and one α-proton can only be explained by hydrogen addition on the double bond of the pyrimidine ring. This assignment is supported by the direction cosines associated with the principal values of the splitting tensors. As in the case of the abstraction radical the absence of significant rearrangements of the ring structure on radical formation is assumed implicitly.

Addition on C(5) as shown in structure **2** and not on C(6) is proven by the values of the direction cosines obtained by fitting the theoretical curves to the experimental points as shown in Fig. 10 and comparison with the corresponding values of the crystal structure. A detailed analysis of the errors involved reveals that addition on C(6) cannot be reconciled with the experimental results if substantial molecular rearrangements are excluded.

This conclusion is supported by the observed minor splittings which are attributed to interaction of the unpaired electron with the N(1) nucleus and the attached methyl group. Theoretical considerations of addition at C(6) suggest that unpaired spin density should reside on N(3) in that case while no splitting should be visible in the *ab*-plane due to the absence of spin polarization and dipole-dipole coupling. Since such splitting has been found experimentally parallel to *b* as has been described above, this is regarded as evidence in favour of addition on C(5).

Finally, the spin density at the C(6) atom is determined from the isotropic α-splitting as $\varrho = 0.74$, in agreement with HMO-calculations yielding a spin density of about 0.73 at C(6) for hydrogen addition at C(5) but only about 0.65 at C(5) for addition at C(6).

Radical concentrations

In addition to qualitative studies quantitative measurements of radicals produced by irradiation have been made. After irradiation at 77 °K the crystal axis *c* was oriented parallel to the magnetic field in order to take advantage of the minimal interference between the spectra of the two types of radicals and the radical pairs at this direction. At each temperature plotted the crystal was annealed for 10 min and subsequently recooled for measurement at about 100 °K.

Relative concentrations of the different types of radicals were determined from the first moments of the first derivative spectra recorded following the method of Wyard [14].

A plot of radical concentrations versus increasing temperature is presented in Fig. 11. Since the errors

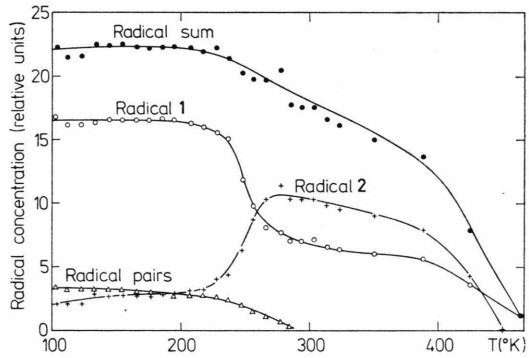

Fig. 11. Relative concentrations of different types of radicals observed and of total sum *versus* temperature of annealing after irradiation at 77 °K.

involved in relative units which are estimated as 20% are smaller than those of absolute determinations the former are used in Fig. 11. In order to obtain the absolute concentration of radicals the relative units of Fig. 11 must be multiplied by a factor of $(5 \pm 2) \cdot 10^{16}$ spins per gram yielding (1.1 ± 0.4)

$\cdot 10^{18}$ spins per gram for the total concentration at 77 °K. This has been obtained with a total dose of about 80 Mrad.

At low temperatures most of the total concentration (about 75%) is made up of the abstraction radical **1** and some 15% of radical pairs whereas the addition radical **2** contributes about 10% only. On heating up to roughly 200 °K these relations are not changed appreciably. Above this temperature a rapid decay of abstraction radical is observed which is accompanied by a similar decrease of radical pairs and an increase of addition radical **2**.

At 280 °K about half the original amount of abstraction radical is left which decays less rapidly at even higher temperatures while the radical pairs have disappeared completely. The concomitant growth of addition radical **2** balances the decay of abstraction radical within experimental limits of error leaving the total concentration nearly unaffected. At room temperature the addition radical has reached about 60% of the total concentration. The same ratio was obtained with a low dose of 150 krad at 77 °K and on irradiation at room temperature.

Above 300 °K all concentrations decrease slowly and essentially proportional to each other up to 400 °K. Above this temperature both types of radicals are becoming less stable but the addition radical significantly more so. At about 460 °K radical **2** has completely vanished and only a fraction of radical **1** is left.

Radical reactions

The rapid change of radical concentrations around 250 °K is considered as a transformation of about half the amount of abstraction radical **1** into addition radical **2**. A simple pathway for this sum reaction would be provided by two consecutive steps: (1) Formation of a covalent link between the radical group of **1** and a neighbouring non-radical molecule thereby splitting off a hydrogen atom and (2) addition of the atomic hydrogen to a non-radical molecule under formation of radical **2**.

The result that only half but not all of the abstraction radical takes part in reaction (1) has been found equally at high and low doses. It could be connected with the spatial relations of radical groups and non-radical molecules. Minor rearrangements of the former should be allowed for. Obviously, the radical molecules of pairs cannot survive this type of reaction in common, whereas a fraction of those abstraction radicals that escapes reaction (1) is stable even at higher temperatures than the addition radical.

* *Note added in proof:* The appearance of two groups of lines may also be due to second order effects, originating from one type of radicals only, as has been found recently [15].

[1] A. Müller and J. Hüttermann, Ann. New York Acad. Sci., in press.
[2] D. W. Green, F. S. Mathews, and A. Rich, J. biol. Chemistry **237**, 3573 [1962].
[3] D. Weymann, W. Flossmann, and J. Hüttermann, Rev. Sci. Inst. **44**, 241 [1973].
[4] H. A. Farach and C. P. Poole, Jr., Adv. Magn. Resonance **5**, 229 [1971].
[5] H. M. McConnell and J. Strathdee, Molecular Physics **2**, 129 [1959].
[6] M. Katayama and W. Gordy, J. chem. Physics **35**, 117 [1961].
[7] M. Katayama, J. molecular Spectroscopy **9**, 429 [1962].
[8] J. Schmidt and W. Snipes, Radiat. Res. **38**, 274 [1969].
[9] J. Hüttermann, J. F. Ward, and L. S. Myers, Jr., Int. J. Rad. Phys. Chem. **3**, 117 [1971].
[10] J. Hüttermann, Int. J. Radiat. Biol. **17**, 249 [1970].
[11] J. N. Herak and G. Schoffa, Molecular Physics **22**, 379 [1971].
[12] W. Derbyshire, Molecular Physics **5**, 225 [1962].
[13] J. P. Colpa and E. de Boer, Molecular Physics **7**, 333 [1964].
[14] S. J. Wyard, J. Sci. Instr. **42**, 769 [1965].
[15] K. Minakata and M. Iwasaki, Molecular Physics **23**, 1115 [1972].